



LETTER

## Coexistence, mixing and fluctuation of nuclear shapes

To cite this article: R. Budaca and A. I. Budaca 2018 *EPL* **123** 42001

View the [article online](#) for updates and enhancements.

# Coexistence, mixing and fluctuation of nuclear shapes

R. BUDACA<sup>1,2(a)</sup> and A. I. BUDACA<sup>1</sup><sup>1</sup> “Horia Hulubei” National Institute for Physics and Nuclear Engineering - Str. Reactorului 30, RO-077125, POB-MG6 Bucharest-Măgurele, Romania<sup>2</sup> Academy of Romanian Scientists - 54 Splaiul Independenței, Bucharest, RO-050094, Romania

received 1 August 2018; accepted in final form 28 August 2018

published online 7 September 2018

PACS 21.60.Ev – Collective models

PACS 21.10.Re – Collective levels

PACS 27.50.+e –  $59 \leq A \leq 89$ 

**Abstract** – The coexistence between near-spherical and well-deformed shapes in nuclear systems is studied by a schematic collective model employing a double-minimum phenomenological potential with an accounted centrifugal contribution from the kinetic energy. The quantum tunneling between the two deformation minima depends on the characteristics of the separating barrier and is gauged by the density probability distribution of deformation in the ground and excited states. Various degrees of overlap between the two states are associated to shape coexistence with and without mixing or to simple shape fluctuation phenomena. The effect of the interaction between deformation configurations on the transition observables is exemplified on the <sup>76</sup>Kr nucleus.

Copyright © EPLA, 2018

**Introduction.** – Most nuclei exhibit shape coexistence of some degree [1]. The term is however reserved to coexistence between few very distinct shapes such as spherical, prolate, oblate, triaxial which arise as minima in potential energy curves mapped from microscopic input [2]. The way in which it manifests depends on the interaction between the competing shapes [3]. Completely separated deformation configurations lead to distinct non-interacting band structures with clear characteristics of their associated shape. Whereas mixed shape configurations are harder to identify from the energy levels, but are usually accompanied by unusually strong inter-band transitions [1,4].

The presence of stable microscopic configurations with different deformations does not necessarily imply a shape coexistence in its usual sense. Indeed, allowing shape fluctuations, the distinction between the supposedly coexisting shapes vanishes in the competition between the stability of the microscopic configurations and the collective excitations. Therefore, strong shape fluctuations as well as shape coexistence with or without mixing are consequences of multiple stable deformation minima in the energy. The question which arises is what conditions distinguish these situations and when it is possible to do so. It is clear that mixing between shapes plays an important role. As coexisting shapes are described by separate min-

ima in the potential energy, their mixing can then be understood as a quantum tunneling through their separating barrier [3]. The effect of the barrier characteristics on the mixing through quantum tunneling and shape fluctuations can be studied with a schematic model based on the collective Bohr Hamiltonian (BH) [5] with a double-well potential in the relevant shape variable.

**Theoretical formalism.** – For well-deformed nuclei, the collective  $K^\pi = 0^+$  states of angular momentum  $L$  can be described by the approximate differential equation [6]

$$\left[ -\frac{1}{\beta^4} \frac{\partial}{\partial \beta} \beta^4 \frac{\partial}{\partial \beta} + \frac{L(L+1)}{3\beta^2} + v(\beta) \right] \Psi(\beta) = \epsilon^\beta \Psi(\beta), \quad (1)$$

for the  $\beta$  shape variable which describes the deviation of the nuclear shape from sphericity. The simplest potential which can achieve simultaneous spherical and deformed minima and satisfy the necessary symmetry restrictions, is the sextic potential. Due to the scaling properties of eq. (1), it can be defined using only two parameters as  $v(\beta) = \beta^2 + a\beta^4 + b\beta^6$ . Such a potential has two minima only if  $a < 0$  and  $b > 0$ . Making the change of function  $\Psi(\beta) = \psi(\beta)/\beta^2$  one can express the differential equation in a one-dimensional Schrödinger form for an effective potential  $v_{eff}(\beta) = 2/\beta^2 + \beta^2 + a\beta^4 + b\beta^6$ . The centrifugal contribution has the effect of raising and displacing the spherical minimum of the original potential  $v(\beta)$  (see fig. 1). Depending on the values of parameters  $a$  and  $b$ ,

<sup>(a)</sup>E-mail: rbudaca@theory.nipne.ro

the less deformed minimum can vanish completely in the effective potential, reducing it to a simple potential well yet with an un-regular inner wall. This explains why the  $\beta$  density probability distribution corresponding to a sextic potential with degenerated minima fragments only for higher barriers which keep the less deformed minimum [7]. Here we consider few cases where instead the effective potential has two degenerated minima. The energies and wave functions of (1) for such potentials are obtained by a diagonalization using the basis states

$$\tilde{\Psi}_{\nu n}(\beta) = \frac{\sqrt{2}\beta^{-\frac{3}{2}}J_{\nu}(\alpha_n\beta/\beta_W)}{\beta_W J_{\nu+1}(\alpha_n)}. \quad (2)$$

$J_{\nu}$  are Bessel functions of the first kind with  $\nu = \sqrt{9/4 + L(L+1)}/3$  and  $\alpha_n$  are their zeros associated to the boundary conditions for a suitably chosen limiting value  $\beta_W$  which encompass the relevant part of the potential  $v(\beta)$  [8]. The boundary value  $\beta_W$  is determined so that to achieve a satisfactory convergence for all considered energy states for a given dimension of the diagonalization basis [7]. We calculated the energies and wave functions for few instances of the sextic potential, whose effective potential exhibits two degenerated deformation minima. A summary of the results is given in fig. 1. Under the restriction of degenerate minima, the barrier of the effective potentials varies from high and thick to low and thin.

**Numerical analysis.** – For sufficiently high barriers, deformation probability distributions for the ground state and the  $0^+$  excited state are localized in the large and respectively low deformation minimum of the effective potential. Such a distribution of states' deformation was also reported before for high barrier phase transitional potentials [9]. The corresponding states are completely separated with understandably different scales of rotational excitations built on them. This scenario is consistent with the more popular definition of the shape coexistence in nuclei based on the emergence of non-interacting bands with strikingly different shape characteristics [1]. The stand alone nature of the two bands in this approach is demonstrated also by the extremely small monopole matrix element which is a convenient measure of the states mixing [4].

As the barrier decreases, both in height and in thickness, the two deformation configurations start to interact due to tunneling between the two potential wells. At some point, both  $0^+$  states exhibit a two-peak probability distribution with almost mirrored shapes. A similar situation arises in symmetric double-minimum tunneling used in molecular physics [10] or in the recent description [11,12] of the transition from chiral vibration to static chirality in nuclei. Although in both cases, the peaks are symmetrical due to the symmetry of the potential. Apparently, the effective potential from the present case is approximately symmetrical with respect to the position of the barrier. However, the total wave function is not, as well as the mass tensor of

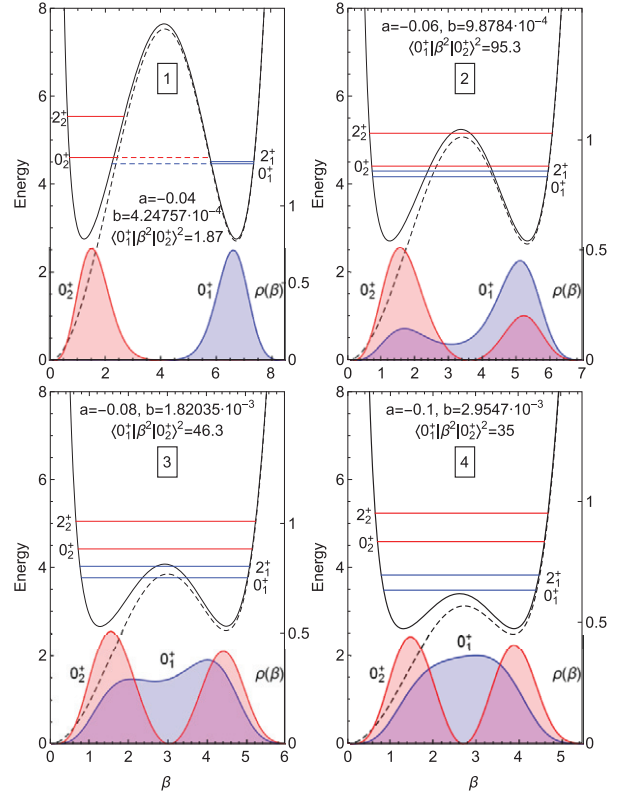


Fig. 1: (Colour online) Effective (solid) and original (dashed) collective potentials as well as the probability distribution corresponding to the first two  $\beta$  excited states are plotted as a function of  $\beta$ . The energy levels  $0^+$  and  $2^+$  belonging to the ground band and  $\beta$  excited band are shown using the same arbitrary units of the potential curves.

the BH kinetic operator. Nevertheless, the clear double-peak shape suggests that both  $0^+$  states can be described with a sizable percentage either by a small or by large deformation associated to the two effective potential minima. In this case, one says that two deformation configurations coexist in the same system as well as in the same state. The situation depicts the phenomenon of shape coexistence with mixing [1], and is shown to generate extremely high monopole strengths between mixed states [4]. The same happens in the present approach due to a maximal overlap between the deformation probability distributions of the  $0^+$  states [13]. Note, however, that although shape mixing will indubitably lead to large monopole strengths, the vice versa is not necessarily true as there are other mechanisms with similar effects.

Decreasing further the barrier but still having the ground state below the barrier, the two deformation probability peaks of the ground state start to merge, remaining however distinguishable. While for the  $0_1^+$  state, the two bell profiles remain separated with their heights more equalized. But when the ground state is above the barrier, the latter starts to be ignored such that one obtains an extended single-peak deformation probability distribution for the ground state. The separated peaks for the

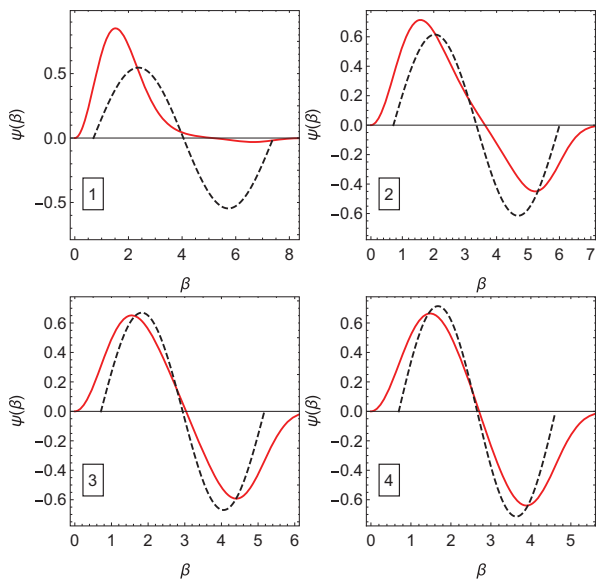


Fig. 2: (Colour online) First-excited  $\beta$  wave function  $\psi(\beta) = \beta^2 \Psi(\beta)$  corresponding to the cases of fig. 1 given as a function of the  $\beta$  shape variable. Solid lines are the results of the present diagonalization, while the dashed lines depicts a freely oscillating deformation in an effective potential approximated as a displaced infinite square well.

excited  $0^+$  state are now equally high and can be regarded as turning points for a  $\beta$  vibration. This is an example of shape fluctuations usually found in mid-shell nuclei, whose extensive valence space generates a multitude of coherent excitations which can be accounted for by a flat collective potential [14]. The last two cases show the transition between shape coexisting with strong mixing and plain shape fluctuation. Although analytically similar, the two phenomena have distinctive behaviour of key observables. For example one would expect a sharp decrease in monopole strength when going from a two-peak to an extended single-peak deformation probability distribution for the ground state.

The excited state in this formalism is obviously beyond the traditional  $\beta$  vibration [15] interpretation. It includes it as a special case when the separating barrier is ignorably small and the ground-state wave function loses its double-peak contour. On the one hand, when the energy of the second  $0^+$  state is below the barrier, as in the cases 1 and 2 of fig. 1, one cannot speak of a vibration in the classical sense between the deformations of the two minima. The potential wells in this situation interact with each other only by tunneling, which does not have a classical counterpart. On the other hand, one can consider the barrier as a probabilistic hindering of the free vibration of the deformation between the inner and outer potential walls. That is, through tunneling there is still possible to have a complete oscillation between the two deformation minima. This interpretation is supported by the persistent presence of a node in the wave function of the  $\beta$  excited state despite sizable separation between the two potential wells.

This can be observed in fig. 2, where one also make a comparison with the  $\beta$  excited wave function corresponding to a freely fluctuating deformation in an infinite square well effective potential confined between the intersection points of the  $0_2^+$  energy level with the exact effective potential. This reminds us of the confined  $\beta$ -soft model (CBS) [16]. However, the same approximation is employed here for the effective potential. The comparison between the two wave functions is meant to show the departure of the present model from the usual  $\beta$  vibrational picture. The extension of the exact wave function beyond the boundaries of the approximated square well is due to its rounded corners and should not be counted as distinctive features of the present formalism. The positions of the maximum and minimum of the wave function is however unaffected by this approximation. Despite the node in the exact wave function, the two pictures are quite distinct for the first two cases. Besides the asymmetry of the positive and negative values, the exact wave functions for these situations exhibit also a slower transition between positive and negative values with a shifted position of the node. As was expected, a good matching is obtained for the last two cases where the vibrational energy state is above the barrier. There are still some differences, which are most obvious at the edges. More precisely, the critical points of the exact wave function are shifted towards the edges. This is ascribed to the presence of the minima near the turning points of the traditional  $\beta$  vibration. The effect subsides when the minima become shallower, and the barrier can be safely ignored. Consequently, the vibrational character of the  $0_2^+$  state is stronger for a higher degree of mixing between the coexisting deformation configurations.

**Experimental realization.** – As an illustrative example, one considered here the nucleus of  $^{76}\text{Kr}$  which is known for its shape coexisting behaviour [17,18]. Contrary to its lighter isotopic neighbors which exhibit a prolate-oblate shape coexistence, one of its coexisting shapes is predominantly spherical while the other dominant shape is prolate [17,19–23]. This is well suited for the present model, which is based on the fact that the nuclear shape is very stiff against adiabatically decoupled fluctuations of the  $\gamma$  shape variable [6]. The available data on the ground band and  $K^\pi = 0^+$  excited band energies were fitted with the model's diagonalization results. The fitted values of the free parameters  $a = -0.07314$  and  $b = 1.5062 \cdot 10^{-3}$  fall into the picture described between the second and third graphs of fig. 1 for shape coexistence with mixing. The same parameters are used to calculate the theoretical  $E2$  transition probabilities as well as the monopole strength connecting the  $0^+$  states using the recipe of ref. [7]. The agreement between energy levels is satisfactory. The reproduction of the electromagnetic properties is however the real test of the model. As can be seen in fig. 3, the low-lying ground-state to ground-state transitions are well described by theory. The in-band transition  $2_2^+ \rightarrow 0_2^+$  from the excited band is overestimated probably due to

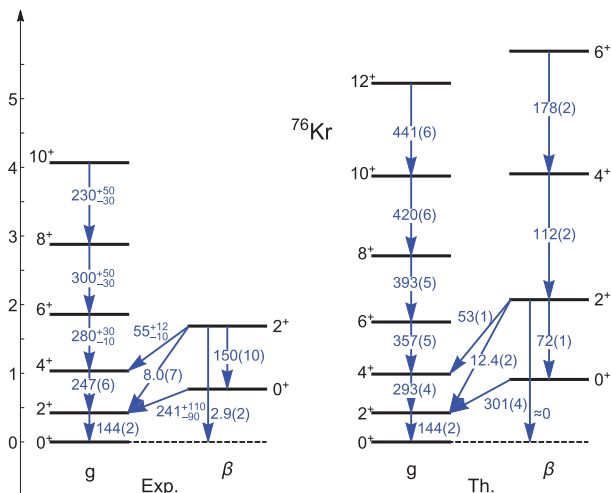


Fig. 3: (Colour online) Theoretical and experimental [18] energy spectra for  $^{76}\text{Kr}$  including only  $K^\pi = 0^+$  states. The energy scale of theoretical predictions is fixed to reproduce the experimental energy of  $2_1^+$  state, while the theoretical  $B(E2)$  values are scaled to the experimental value of the  $2_1^+ \rightarrow 0_1^+$  transition. Energy levels are given in MeV and  $B(E2)$  values in  $e^2b^2$ .

the higher theoretical excitation energy. An especially good agreement between theory and experiment is obtained for all the inter-band transitions, whose high values are the result of a sizable overlap between the wave functions of the two bands. Note that this is achieved mainly due to a double-peak distribution of deformation in the ground state. Scaling the  $\beta$  variable so that the position of the highest peak of the deformation probability distribution in the ground state is equal to the tabulated quadrupole ground-state deformation [24], one obtains the theoretical estimation [7] of the monopole strength  $\rho(E0) = 87.14 \cdot 10^{-3}$ . Comparing it to the measured value of  $79(11) \cdot 10^{-3}$  [25], one can see that the good agreement with experiment for the inter-band transition is also valid for monopole strength.

**Outlook.** – In conclusion, we obtained for the first time a collective ground state with a double peak structure. The two peaks correspond to the deformation minima of the effective collective potential and arise due to strong mixing between the two coexisting deformation configurations. Such a structure of the ground state leads to an enhanced overlap with the traditional two-peak excited state of  $\beta$  vibration. This translates into very high inter-band electromagnetic transitions. The hypothesis was positively tested on the shape coexisting  $^{76}\text{Kr}$  nucleus.

\*\*\*

This work was supported by a grant of Ministry of Research and Innovation, CNCS - UEFISCDI, project No. PN-III-P1-1.1-TE-2016-0268, within PNCDI III.

## REFERENCES

- [1] HEYDE K. and WOOD J. L., *Rev. Mod. Phys.*, **83** (2011) 1467.
- [2] LI Z. P., NIKŠIĆ T. and VRETENAR D., *J. Phys. G: Nucl. Part. Phys.*, **43** (2016) 024005.
- [3] MATSUYANAGI K., MATSUO M., NAKATSUKASA T., YOSHIDA K., HINOHARA N. and SATO K., *J. Phys. G: Nucl. Part. Phys.*, **43** (2016) 024006.
- [4] WOOD J. L., ZGANJAR E. F., DE COSTER C. and HEYDE K., *Nucl. Phys. A*, **651** (1999) 323.
- [5] BOHR A. and MOTTELSON B. R., *Nuclear Structure*, Vol. **2** (Benjamin, Reading, Mass.) 1975.
- [6] IACHELLO F., *Phys. Rev. Lett.*, **87** (2001) 052502.
- [7] BUDACA R., BUGANU P. and BUDACA A. I., *Phys. Lett. B*, **776** (2018) 26.
- [8] TAŞELI H. and ZAFER A., *J. Comput. Appl. Math.*, **95** (1998) 83.
- [9] MACEK M. and LEVIATAN A., *Ann. Phys. (N.Y.)*, **351** (2014) 302.
- [10] HARMONY M. D., *Chem. Soc. Rev.*, **1** (1972) 211.
- [11] CHEN Q. B., ZHANG S. Q., ZHAO P. W., JOLOS R. V. and MENG J., *Phys. Rev. C*, **94** (2016) 044301.
- [12] BUDACA R., *Phys. Rev. C*, **98** (2018) 014303.
- [13] BONNET J., KRUGMANN A., BELLER J., PIETRALLA N. and JOLOS R. V., *Phys. Rev. C*, **79** (2009) 034307.
- [14] CASTEN R. F. and CAKIRLI R. B., *Phys. Scr.*, **91** (2016) 033004.
- [15] GARRETT P. E., *J. Phys. G: Nucl. Part. Phys.*, **27** (2001) R1.
- [16] PIETRALLA N. and GORBACHENKO O. M., *Phys. Rev. C*, **70** (2004) 011304(R).
- [17] BENDER M., BONCHE P. and HEENEN P.-H., *Phys. Rev. C*, **74** (2006) 024312.
- [18] CLÉMENT E. *et al.*, *Phys. Rev. C*, **75** (2007) 054313.
- [19] GAUDEFROY L. *et al.*, *Phys. Rev. C*, **80** (2009) 064313.
- [20] FU Y., MEI H., XIANG J., LI Z. P., YAO J. M. and MENG J., *Phys. Rev. C*, **87** (2013) 054305.
- [21] YAO J. M., HAGINO K., LI Z. P., MENG J. and RING P., *Phys. Rev. C*, **89** (2014) 054306.
- [22] RODRÍGUEZ T. R., *Phys. Rev. C*, **90** (2014) 034306.
- [23] NOMURA K., RODRÍGUEZ-GUZMÁN R., HUMADI Y. M., ROBLEDO L. M. and ABUSARA H., *Phys. Rev. C*, **96** (2017) 034310.
- [24] Data retrieved from the NUDAT Online Data Service (<https://www.nndc.bnl.gov/nudat2>).
- [25] GIANNATIEMPO A. *et al.*, *Phys. Rev. C*, **72** (2005) 044308.